



Interactive effects of climate variability and human activities on blue and green water scarcity in rapidly developing watershed

Jie Liang^{a, b, *}, Qiang Liu^{a, b}, Hua Zhang^{c, **}, Xiaodong Li^{a, b}, Zhan Qian^d, Manqin Lei^{a, b}, Xin Li^{a, b}, Yuhui Peng^{a, b}, Shuai Li^{a, b}, Guangming Zeng^{a, b}

^a College of Environmental Science and Engineering, Hunan University, Changsha, 410082, PR China

^b Key Laboratory of Environmental Biology and Pollution Control, Ministry of Education, Hunan University, Changsha, 410082, China

^c School of Engineering and Computing Sciences, Texas A&M University-Corpus Christi, Corpus Christi, 78412, USA

^d Dongting Lake Research Center, Hunan Hydro & Power Design Institute, Changsha, 410007, China

ARTICLE INFO

Article history:

Received 30 November 2019

Received in revised form

17 April 2020

Accepted 19 April 2020

Available online 23 April 2020

Handling Editor: Cecilia Maria Villas Bôas de Almeida

Keywords:

Blue water

Green water

Xiangjiang River Basin

SWAT

Climate change

Land use change

ABSTRACT

Quantifying the spatiotemporal distribution of water resources is still a key constraint on water resources management against the background of climate change and human activities. To investigate the interaction of climate variability and human activities on blue and green water scarcity (BW and GW-scarcity), the soil and water assessment tool (SWAT) model was used to simulate BW and GW-scarcity and its spatiotemporal distribution under scenarios of single or combined land-use change and climate variability. Multivariate statistical methods were used to identify the main factors affecting blue/green water and confirm the hot spots of water management. Taking the rapidly-developing Xiangjiang River Basin (XRB) in China as an example, where the urbanization rate increased from 42.15% in 2008 to 56.02% in 2018, the results showed that BW-scarcity was mainly affected by precipitation ($r = 0.425$) and population ($r = -0.612$), while GW-scarcity was mainly affected by agriculture ($r = 0.429$) and urban land ($r = -0.593$). The hot spot areas of blue and green water (BW and GW) shortage accounted for 29.7%, 4.6% and 3.4% of the total area in the lower reach, middle reach and upper reach of XRB, respectively. The rapid development of urbanization in the lower reach of the XRB caused serious shortage of BW and GW resources. This study would provide useful information for water resources management in corresponding human-water system. Future research should focus on how to optimize water resource allocation upstream and downstream of the basin.

© 2020 Elsevier Ltd. All rights reserved.

1. Introduction

Freshwater is important to maintain the sustainable development of ecological balance and anthropogenic activities. Under the influence of climate variability, population growth and changing lifestyles, water scarcity has become critical challenge worldwide over the past few decades (Du et al., 2018; Hua et al., 2015; Liang et al., 2018). It has been reported that human water demand increased almost eight times as a result of doubled global population and improved living standards in the past 100 years (Veldkamp

et al., 2017). Therefore, in order to improve the effective utilization of water resources, the evaluation and management of water resources are mainly concentrated in BW and GW, which will help policymakers to manage water resources rationally (Liang et al., 2009; Yuan et al., 2019; Zhao et al., 2016). The BW is simulated by combining both groundwater storage and surface water, while GW represents the sum of soil water content and actual evapotranspiration (Johansson et al., 2016; Zhao et al., 2016). The BW is mainly used for industrial production and agricultural irrigation and the GW maintains crop production, forestry and terrestrial ecosystems (Schyns et al., 2015). Therefore, the study of BW and GW plays a vital role in maintaining ecosystem stability and global food security, and has a positive effect on optimizing water resources management in the basin (Zhao et al., 2016).

With the influence of population growth and climate variability, the BW and GW-scarcity have become severe. The BW and GW-scarcity are important evaluation indexes that are the water

* Corresponding author. College of Environmental Science and Engineering, Hunan University, Changsha, 410082, PR China.

** Corresponding author.

E-mail addresses: liangjie@hnu.edu.cn (J. Liang), Hua.Zhang@tamucc.edu (H. Zhang).

consumption divided by the available water, which could be used to identify geographic hotspots in water stress areas. To help balance competing demands such as agricultural water, domestic water and other uses, water managers often use hydrological models to rationally allocate blue/green water resources (Veettil and Mishra, 2016). Since Faramarzi et al. (2009) first proposed the concept of BW and GW, a large number of studies have examined the blue/green water resources. For instance, Rost et al. (2008) used the Lund-Potsdam-Jena managed Land (LPJmL) model to quantify the historic blue/green water consumption in global irrigated agriculture over 30 years. The SWAT was often used to simulate the effects of land-use change and climate change on hydrology (Niraula et al., 2015; Noori and Kalin, 2015; Shrestha et al., 2017). Many previous studies proved that the SWAT was effective in simulating land-use and climate change on hydrological change in many regional watersheds of the world (Du et al., 2018; Veettil and Mishra, 2018; Zhou et al., 2013). Shrestha et al. (2017) used the SWAT model to simulate the influence of climate variability on the BW and GW in the Athabasca River Basin in Canada. Du et al. (2018) quantified the relative effects of land use and climate changes on the BW and GW dynamics over 80 years (1935–2014). These studies discussed the effects of land-use change and climate variability on the spatio-temporal distribution of BW and GW in the past period, but these studies did not quantify the key factors affecting BW and GW shortage and hotspots in water resources management, then were lack of consideration on future land use and climate scenarios, and did not explain the underlying mechanisms behind the changes of BW and GW. Results showed that the change of BW and GW may be attributed to the notable precipitation change and land use change, respectively. Land use change and climate variability have important effects on the spatiotemporal distribution of blue/green water resources. For example, urban development leads to an increase in impervious surface (Giri et al., 2018) and in turn reduces groundwater recharge, while climate change (such as temperature and precipitation) affects streamflow and evapotranspiration. The spatial distribution of BW was mainly affected by population and climate change, and the spatial distribution of GW was mainly affected by agricultural and urban land (Veettil and Mishra, 2018). The influence of land use and climate change on the spatiotemporal distribution of BW and GW is synergistic or antagonistic, that depends on the actual social development and geographical conditions of the study area. However, the joint and relative effects of future climate change and land use on spatiotemporal distribution of BW and GW, as well as its scarcity, are still poorly understood, despite its recognized importance (Giri et al., 2018). When it comes to the BW and GW-scarcity, which is more important for water resource management in the rapid developing region in the scope of corresponding human-water systems, the problems are more complicated, for more social factors may be incorporated in the system.

The Xiangjiang River is one of the largest tributaries of the Yangtze River and the main source of water supply for the Hunan Province (Chen et al., 2018; Zuo et al., 2015). The XRB is a typical agricultural area and urbanization has developed rapidly in recent years, which the urbanization rate has increased from 42.15% in 2008 to 56.02% in 2018 (An et al., 2019). With the rapid development of urbanization, the amount of water withdrawal increased significantly and the ecological water demand reduced greatly in the past 40 years, which negatively affected the sustainable development of society. Therefore, in order to improve the effective use of BW and GW and help decision makers manage water resources reasonably, studying the blue/green water resources in the XRB is necessary for facilitating the sustainable use of water resources and protecting the stability of river ecosystems in central China (Zhao et al., 2016; Zuo et al., 2015). The objectives of this

work are to: (1) calibrate and validate SWAT model on a monthly time step with the uncertainty analysis, (2) quantify the single and combined effects of future land-use change and future climate variability on blue/green water resources and their scarcity in XRB and (3) analyze the key factors affecting the change of BW and GW-scarcity.

2. Study area and data

2.1. Study area

The 94,660-km² XRB (Fig. 1) is located in Hunan Province in central China (24°38'06" N–28°40'23" N and 110°30'14" E–114°15'00" E). It is a tributary of the Yangtze River with an elevation of 21–1953 m which is gradually decreasing from southwest to northeast. This region has an East Asian monsoon climate. The annual average temperature is 17.2 °C and average annual precipitation is 1450 mm. Precipitation from April to June accounts for 40–45% of the annual precipitation, compared to 18% from July to September. Since reform and opening up, water supply and demand was unbalanced among available water resources, economic society and environment, which led to the growing conflicts among different water users in XRB. There was a serious shortage of water resources in China, that per capita water resources is only about 25% of the world's per capita water resources (Hoekstra and Mekonnen, 2012). Accordingly, an accurate assessment of water resources in the XRB is of great significance to water resources planning and management.

2.2. Data

The inputs of the SWAT model included topography, soil, land use, and weather data. We used the 90-m SRTM data obtained from Geospatial Data Cloud (2018) for delineating streams and sub-basins. The data of soil and land use were used to generate the Hydrologic Response Units (HRUs) in the SWAT. The observed daily streamflow from 2008 to 2017 at the Xiangtan, Zhuzhou, Hengshan, Hengyang and Guiyang hydrological stations were simulated by using the SWAT model (Faramarzi et al., 2013). The per capita comprehensive water consumption in 2050 was assumed to be the same as that of 2015. The population per county in 2050 was estimated based on average fertility and mortality trends from 2015 to 2018, which was obtained from Hunan Provincial Bureau of Statistics. The redundancy analysis (RDA), cluster analysis (CA), and Pearson correlation analysis (PCA) required blue/green water scarcity, population, urban land, agriculture, forest, precipitation, and temperature data. And the last five of indexes came from the output of SWAT model. The blue/green water and blue/green water scarcity were detailed in section 3.1 below. The applications and sources of these data were listed in Table 1. The abbreviations for each phrase in an alphabetical order were listed in Table S4 in Supporting Information.

3. Methodology

As shown in Fig. 2, the research framework of this study consisted of three main components: 1) establishing the SWAT hydrological model and predicting the spatial distribution of blue/green water resources, 2) building future land use and climate scenarios and calculating the blue/green water resources in different scenarios, and 3) determining the key factors which affects the quantity and distribution of blue/green water resources by using multivariate statistical methods. The data requirements, data sources, and processes were described in detail below.

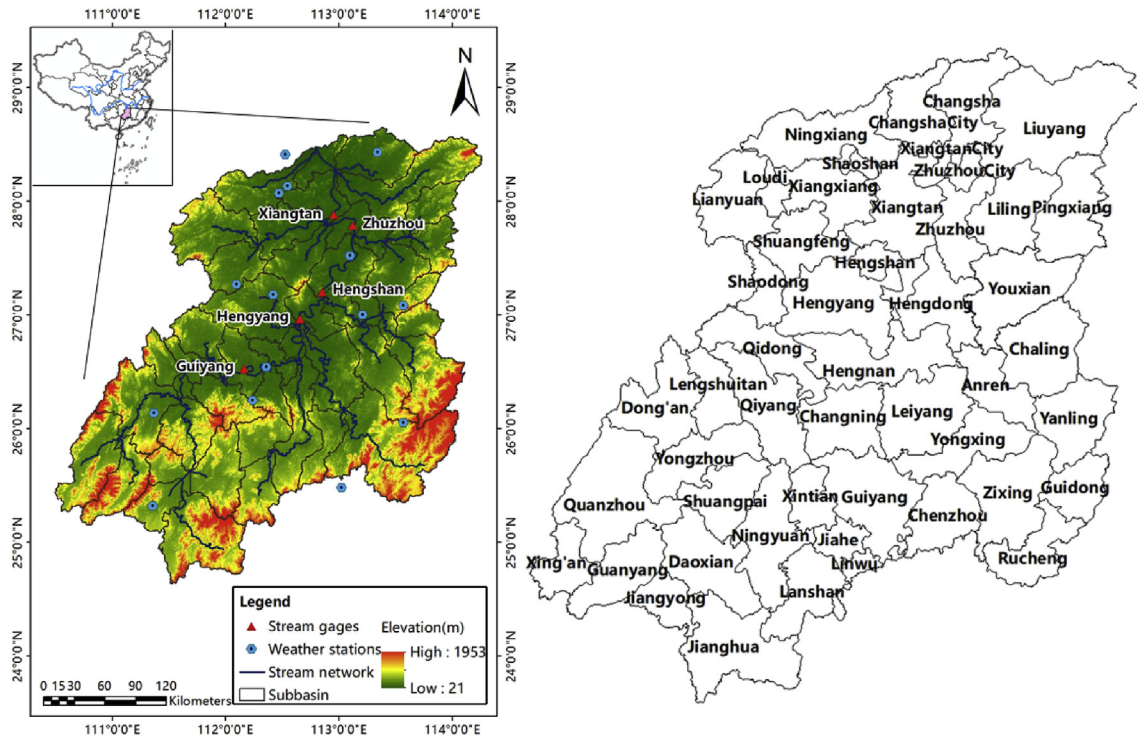


Fig. 1. Location of the study area, hydrological stations and weather stations (Left), and spatial location of counties in the Xiangjiang River Basin (Right).

Table 1
Data used (inputs) for SWAT model development.

Data used	Resolution	Source	Description
Land use	1000m	Resource and Environment Data Cloud Platform	The land use type data layer in 2005 and 2015
Topography	90m	Geospatial Data Cloud ^a	Digital Elevation Model
Soil	1:1000000	Cold and Arid Regions Science Data Center at Lanzhou ^b	The detailed soil composition
Meteorological data	Daily	National Meteorological Information Center	The daily temperature and precipitation from 2006 to 2017
Future climate data	1000 m	Downscaled global climate model (GCM) data from CMIP5 (IPCC Fifth Assessment) ^c	The daily temperature and precipitation in 2050 (average for 2041–2060)
Streamflow data	Daily	Hunan Provincial Department of Water Resources	The streamflow data from 2008 to 2017
Population	Person	Hunan Provincial Bureau of Statistics ^d	Population at the county level in 2015
Per capita comprehensive water consumption	m ³ /year	Hunan Provincial Water Resources Communique ^e	Per capita comprehensive water consumption in 2015

^a Source: <http://www.gscloud.cn/>.

^b Source: <http://westdc.westgis.ac.cn/>.

^c Source: <http://www.worldclim.org/>.

^d Source: <http://tjj.hunan.gov.cn/>.

^e Source: <http://slt.hunan.gov.cn/>.

3.1. Hydrologic modeling framework

3.1.1. SWAT model calibration and performance evaluation

The SWAT was a physically-based, semi-distributed hydrological model that was developed by the United States Department of Agricultural (USDA). It operated at daily time steps (Veettil and Mishra, 2018). The model had great advantages of simulating water quality, water quantity and plant growth in different management practices. However, this model required more module data to import and more accurate data was needed, which made it difficult to collect and organize data (Tuo et al., 2018). According to the size of the watershed area and the sub-watershed identification of the SWAT model, we divided the XRB into 53 sub-basins and 354 HRUs in this research. By identifying the attribute conditions of land use and soil at the HRU scale, the model can address the patterns of streamflow and groundwater processes to enhance simulation

accuracy. The water balance equation of the SWAT model is as follows (Awan and Ismaeel, 2014):

$$SW_n = SW_0 + \sum_{k=1}^n (P_{day,k} - Q_{surf,k} - E_{a,k} - W_{seep,k} - Q_{gw,k}) \quad (1)$$

where SW is the soil water content on day k (mm), n is the time (days). $P_{day,k}$, $Q_{surf,k}$, $E_{a,k}$, $W_{seep,k}$ and $Q_{gw,k}$ are precipitation, surface streamflow, actual evapotranspiration, seepage, and return flow, respectively.

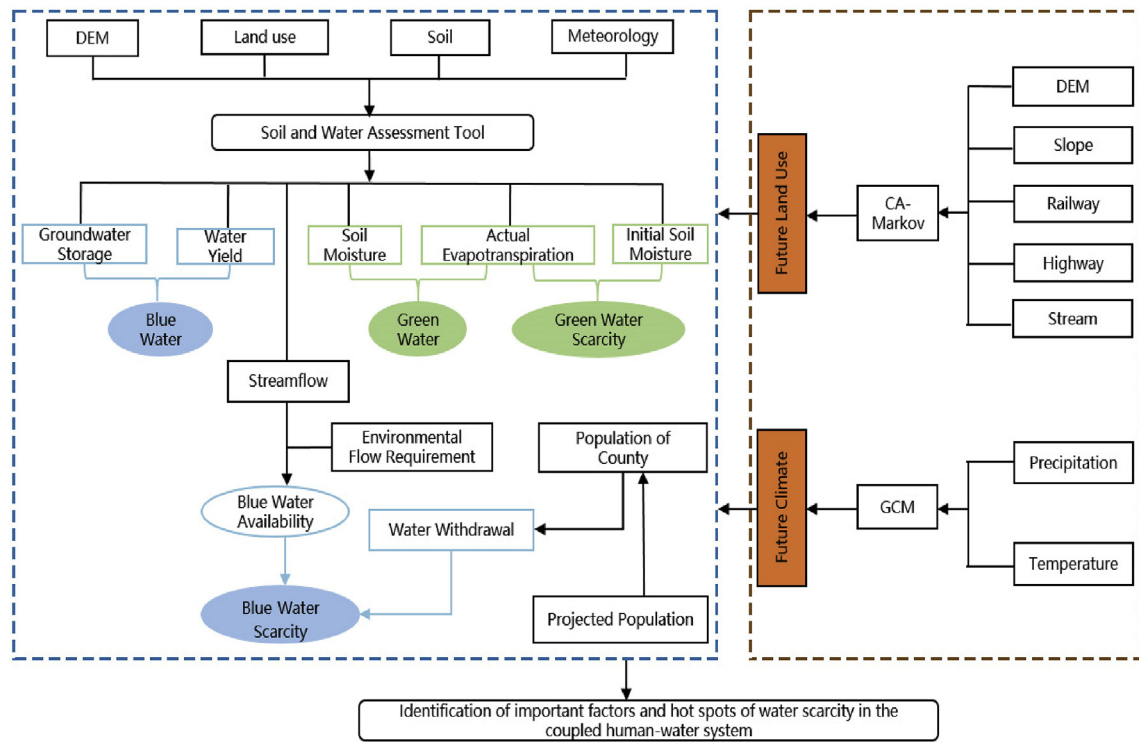


Fig. 2. Schematic of integrated modeling framework for blue/green water analysis in the Xiangjiang River Basin.

SWAT Calibration and Uncertainty Programs (SWAT-CUP) is used to calibrate the parameters of the SWAT model (Wang et al., 2019). By adjusting the model parameters, the accuracy of the model can be improved to better reflect the hydrological process of interest. The SWAT simulations of XRB in this study consisted of the warming-up period (2006–2007), the calibration period (2008–2012), and validation period (2013–2017). Streamflow observations at five hydrological stations in Xiangtan, Zhuzhou, Hengshan, Hengyang, and Guiyang were used for calibration and validation. The coefficient of determination (R^2), Nash-Sutcliffe efficiency coefficients (NS) and percent bias ($BIAS$) were used as measures to evaluate the accuracy of the SWAT model (Wang et al., 2019). Normally the values of R^2 and NS were generally considered to be greater than 0.50, the value of $BIAS$ was less than or equal to $\pm 20\%$, then the SWAT calibration results on a monthly scale were acceptable (Awan and Ismaeel, 2014).

3.1.2. Evaluation of blue water and blue water scarcity

The BW is simulated by combining both groundwater storage and water yield (WYLD). Groundwater storage is the difference between total amount of water recharge to aquifers (GW_RCHG) and the amount of water from aquifer that contributes to the main channel flow (GW_Q). Water yield is the amount of water leaving the HRU and entering the main channel (Rodrigues et al., 2015; Veetil and Mishra, 2016). The BW-scarcity is the ratio of the blue water withdrawal to blue water availability (Veetil and Mishra, 2016). The blue water withdrawal is calculated from surface water or groundwater resources.

In this study, the amount of blue water extracted was obtained from county-level water conservancy agencies. The total amount of water withdrawal accounted for 95.6% of surface water and 4.4% of groundwater. Among the different water abstraction sectors, the agricultural irrigation, industrial water and household water use accounted for the largest proportion, accounting for 57.3%, 17.4%

and 15.4%, respectively (Table S3). The total water withdrawal in each county was estimated by multiplying the total population in each county by the per capita comprehensive water consumption. It could be used to simulate the water scarcity in 2050.

As the over exploitation of blue water resources may damage local river ecosystem, the Environmental Flow Requirement which represents that the lowest required streamflow to maintain the healthy ecosystem of stream is equal to 80% of the annual streamflow (Rodrigues et al., 2015; Veetil and Mishra, 2016). More than 20% of the BW being extracted may cause ecological degradation (Veetil and Mishra, 2018).

The calculations for *Environmental Flow Requirement*, *Blue water availability*, and *BW-scarcity* are as follows (equation (2), (3) and (4)) (Giri et al., 2018; Rodrigues et al., 2015).

$$\text{Environmental Flow Requirement} = 0.8 \text{ mean streamflow} \quad (2)$$

$$\text{Blue water availability} = \text{streamflow} - \text{Environmental Flow Requirement} \quad (3)$$

$$\text{BW} = \frac{\text{water withdrawal}}{\text{Blue water availability}} - \text{scarcity} \quad (4)$$

where *streamflow* is the monthly stream flow (m^3/s). *Blue water withdrawal* indicates the combined water consumption of all departments of county n at time t .

3.1.3. Evaluation of green water and green water scarcity

The GW consists of green water storage (soil water content) and green water flow (evapotranspiration). The GW is simulated as the sum of soil water content (SW) and evapotranspiration (ET) (Rodrigues et al., 2015; Schuol et al., 2008).

The GW-scarcity is calculated as the ratio between green water withdrawal and green water availability. The green water withdrawal is stored in the root zone of the soil and is used by plants for evaporation, transpiration or absorption. The green water withdrawal is the actual evapotranspiration that can be acquired from the HRU output of the SWAT model (ET) (Rodrigues et al., 2015; Veetil and Mishra, 2016). The green water availability refers to the amount of soil moisture available for the sustaining crop growth and soil evapotranspiration that represents the initial soil water content. It is also obtained from the HRU output of the SWAT model (SW) to calculate the GW-scarcity. This calculation is as follows (equation (5)) (Giri et al., 2018; Veetil and Mishra, 2018):

$$GW - scarcity = \frac{\text{Green water withdrawal}}{\text{Green water availability}} \quad (5)$$

where *Green water withdrawal* and *Green water availability* represent the green water consumed and the initial soil water content of county n at time t , respectively.

3.2. Future land use and climate change scenarios

To distinguish the single and combined effects of land use and climate change on the water resources of XRB, four scenarios listed below were established in this study (Zuo et al., 2016):

Baseline scenario (S_0): regional climate condition during 2008–2017 and land use pattern of XRB in 2015;

Scenario 1 (S_1): regional climate condition during 2008–2017 and simulated land use pattern in 2050;

Scenario 2 (S_2): downscaled regional climate condition during 2041–2060 and land use in 2015;

Scenario 3 (S_3): downscaled regional climate condition during 2041–2060 and simulated land use in 2050.

Land use in 2050 was simulated by a CA-Markov model (Cellular Automata-Markov), which combined the CA model's ability to simulate spatial complex system changes and the Markov model's advantages in quantitative prediction. Land use maps of 2005 and 2015 were used to calculate the transition probability matrix and then the matrix was used to simulate the land cover map in 2050 (Hou et al., 2019). Based on previous research, we selected seven driving factors, i.e., digital elevation model (DEM), slope, distance to railway station, town, main road, river and permanent water (Liang et al., 2016; Xue et al., 2019). The transition suitability maps of land use change for each land use type was generated by using a multi-criteria (MCE) model. It could improve the accuracy of the simulation result (Hou et al., 2019). The Kappa coefficient was used to evaluate the accuracy of land use data and simulation results. The results showed that the Kappa value was 0.76, suggesting that it can be used for land use prediction in 2050 (Fig. S2).

The climate change scenario in 2050 was the RCP 4.5 (Representative Concentration Pathway) emission scenario at 30 seconds resolution (~1 km) of General Circulation Model (GCM) (average for 2041–2060) in the study (Masud et al., 2019). A statistical downscaling method was used to downscale the CMIP5 data and the change factor approach from statistical downscaling method was applied to generate the regional climate conditions of XRB (Mou et al., 2017).

3.3. Determinating the main factors affecting blue/green water scarcity change

In this research, we studied the spatiotemporal distribution of BW and GW-scarcity in 49 counties of XRB. Under the influences of population, urban land, agriculture, forest, precipitation, and temperature, the change of BW and GW-scarcity in each county varied from 2015 to 2050. To analyze the relationship between BW and GW-scarcity and the above seven environmental factors, the most applied methods to determine the main environmental factors, affecting the change of BW and GW-scarcity, were RDA and PCA, which were realized by Canoco 5.0 and Origin 9.1 software, respectively (Cheng et al., 2018). The positive correlation meant that there was a synergistic relationship between blue/green water scarcity and matched environmental factors, while the negative correlation meant that there was a certain antagonistic relationship between blue/green water scarcity and pairing environmental factors (Liu et al., 2019). In order to analyze whether the environmental factors of these samples were similar, we used CA, which is a statistical method for clustering samples by similarity and various cluster rules, to identify these similar counties to improve water resources management (Charles and Alamsjah, 2019).

4. Results and discussions

4.1. Calibration and validation of the SWAT model

The SUFI-2 algorithm in SWAT-CUP was used to analyze the sensitivity of 8 parameters which were then used for the model calibration (Nilawar and Waikar, 2019) in Table S1 in Supporting Information. The parameters CN2, ALPHA_BF, and CH_N2 were more sensitive than other parameters in the XRB (Chen et al., 2017). Fig. S1 illustrated the calibration and validation results on the five control stations located in lower, middle and upper part of the XRB, respectively. In order to better present the performance of the model simulation, R^2 , NS and relative $BIAS$ were calculated for the streamflow, as shown in Table S2. When $R^2 \geq 0.6$, $NS \geq 0.5$ and $BIAS \leq \pm 20\%$, the model simulation results were considered satisfactory. For Xiangtan Station, the R^2 values for calibration and validation were 0.87 and 0.81, respectively. The NS values were 0.87 and 0.80 and the relative $BIAS$ were -1.7% and 2.3% , respectively. Its overall performance was better than the Hengyang station in the middle reach and the Guiyang station in the upper reach. For these five stations, the hydrological model reasonably simulated streamflow (Xu et al., 2013). Judging from the spatial distribution of these hydrological stations, the results showed that the NS of the downstream station was higher than that of the upstream station. Since the model was calibrated from upstream to downstream, the best simulation of the upstream parameters contributed partly to the next calibration process, improving the simulation results at the downstream station. As we can see from Table S2, the performance of the five control stations attained the requirement, meaning that the SWAT model was well established for XRB region and can be used in further analysis.

4.2. Effects of climate variability and human activities on blue water and blue water scarcity

The spatiotemporal distribution of BW and GW was of great significance for water resources planning. The changes of BW under different scenarios are displayed in Fig. 3. The spatial distribution of BW change was uneven. Under the land use change scenario (Fig. 3a), the decrease of BW was mainly distributed in Liuyang, Changsha and Xiangtan in the lower reach of XRB, Qiyang in the middle reach, and Jianguyong in the upper reach. The maximum

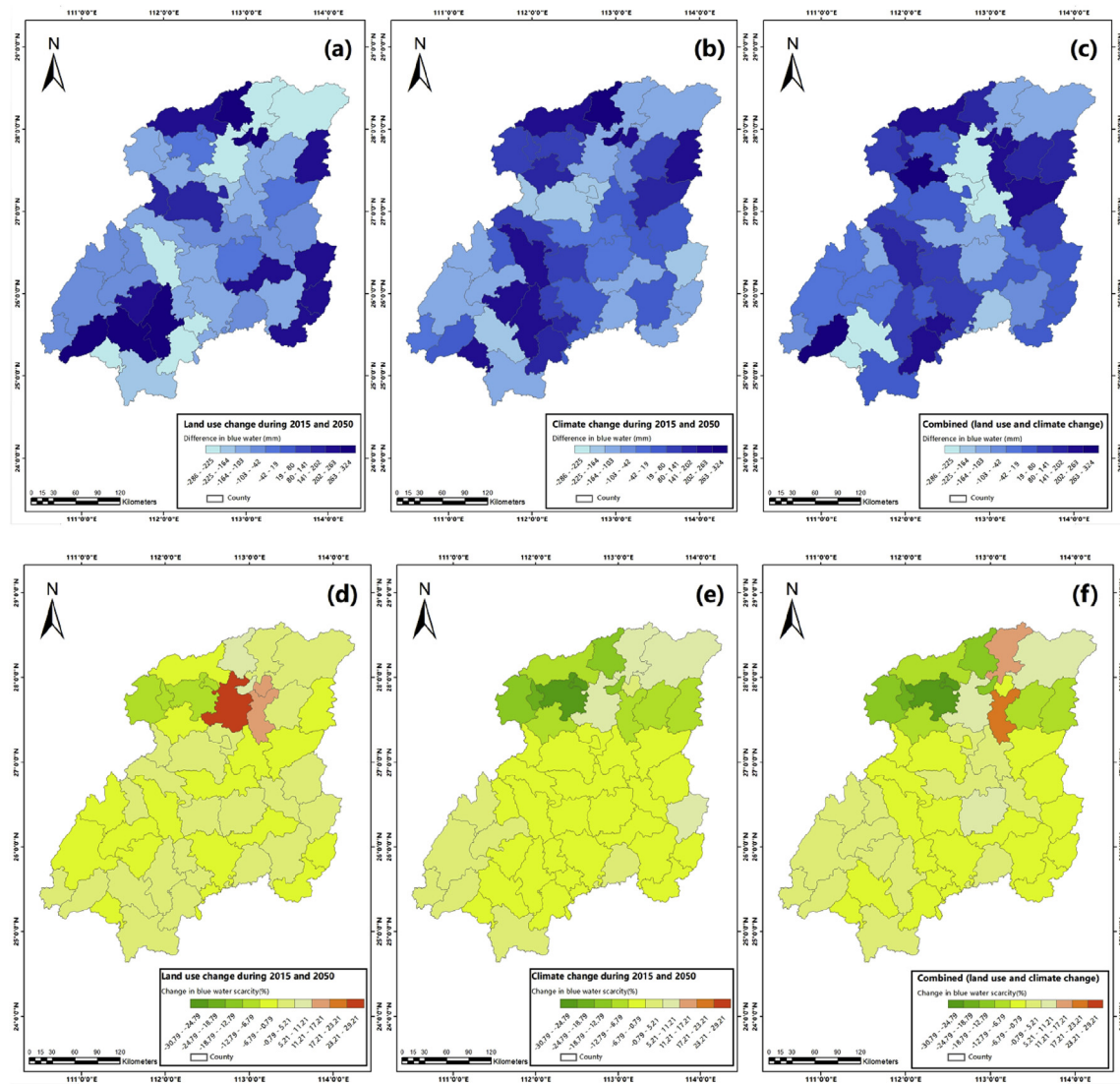


Fig. 3. Changes of the spatial distribution of blue water and blue water scarcity in Xiangjiang River Basin.

reduction of BW in Changsha was 265 mm. The main reason for the change was that the urban expansion in the lower reach which led to increasing impervious surface and greater surface streamflow (Giri et al., 2018). It may also be the increase of cultivated land, which increased the irrigation water consumption. The increase of BW was mainly distributed in Changsha, Xiangtan and Zhuzhou in the lower reach, and Guanyang, Ningyuan in the upper reach. The maximum increase of BW in Ningyuan was 312 mm, which was due to the increase of the forest in the upper reach accordingly (Zang et al., 2012). Under the climate variability scenario (Fig. 3b), the reduction of BW was mainly distributed in Hengyang and Shaodong in the middle reach. The increase of BW was mainly distributed in Ningxiang in the lower reach. The reason for this change was the uneven distribution of regional precipitation in XRB. For the Weihe River Basin of northwest China, the impact of climate change on BW was more pronounced than the impact of land use change on BW. This was different from the results in the XRB, which could be result of the dry climate in northwestern China (Zhao et al., 2016).

Under combined future land use and climate scenarios (Fig. 3c), the decrease of BW was mainly distributed in Changsha, Hengshan

and Xiangtan in the lower and middle reaches, and Jianguyong in the upper reach. The increase was mainly distributed in Ningxiang and Zhuzhou in the lower reach, and Guanyang in the upper reach. For example, in Changsha, the BW was reduced by 265 mm and 154 mm under land-use change scenario and climate variability scenario, respectively, but the BW was reduced by 112 mm under future land use and climate scenario. It could be due to the construction of water diversion projects which reduces the pressure on BW resources. Land use and climate changes were not a simple synergistic effect on BW changes. It could be the combined effects of urban land, agriculture, forests, and precipitation (Veetil and Mishra, 2018; Wang et al., 2015).

To better analyze the BW-scarcity in different regions, Fig. 3 showed the changes in the spatial distribution of BW-scarcity in three scenarios (Veetil and Mishra, 2018). Under the land use change scenario (Fig. 3d), the BW-scarcity change in the lower reach of the XRB was obvious (e.g., Zhuzhou and Xiangtan). The BW-scarcity in Zhuzhou and Xiangtan increased by 14.29% and 26.21%, respectively. Owing to the urban development in Zhuzhou, the population grew rapidly and the water withdrawal increased greatly. In addition, due to the increase of agricultural land in

Xiangtan, the irrigation water demand increased significantly. Under the climate variability scenario (Fig. 3e), the largest reduction in the BW-scarcity in Xiangxiang reached 27.79%. This was probably due to the increase in groundwater storage and water yield caused by precipitation, which in turn increased the blue water availability. Under future land-use and climate scenarios (Fig. 3f), the BW-scarcity in Changsha and Zhuzhou in the lower reach increased significantly. As urban expansion and agricultural land grew, the per capita integrated water consumption increased sharply, resulting in a rapid decline in surface streamflow and groundwater. From the above analysis, it could be concluded that population, agricultural irrigation and precipitation were the three main environmental factors affecting the BW-scarcity change.

4.3. Effects of climate variability and human activities on green water and green water scarcity

The GW played a vital role in the agricultural sector, most of which was carried out through rainwater irrigation systems. The GW was stored in the unsaturated soil layer, which was mainly used for plant growth. Under the land use change scenario (Fig. 4a), the decrease of GW was mainly distributed in Changsha in the lower reach of XRB, and Guidong, Rucheng and Jianghua in the upper

reach. The main reason was that the urban expansion in the lower reach increased the impervious surface and decreased the surface water permeability as well as soil water content; the returning farmland to forest policy in the upper reach promoted the area of forest land, and the trees had deeper roots and higher water storage capacity, which could reduce the green water resources. The increase of GW was mainly distributed in Xiangtan, Liling and Hengdong in the lower and middle reaches, which might be due to the growth of agricultural land. Most crops were shallow-rooted plants and were sensitive to high evapotranspiration environment. This led to the increasing in soil water retention capacity and soil evaporation. Under the climate variability scenario (Fig. 4b), the decrease of GW was mainly distributed in Changsha and Xiangtan in the lower reach. The main reason was the decrease in evaporation due to the increase in impervious surface. The increase of GW was mainly distributed in Liuyang and Pingxiang in the lower reach. The reason for this change may be that the temperature rise led to an increase in crop evaporation and it was also possible that the raising of the precipitation at that time led to an increase in soil water content. For the Savannah River Basin of Southeastern USA, Veetil and Mishra (2018) argued that the changes of climate change patterns had a greater impact on GW. Compared with XRB, it showed that different watersheds had different impacts on GW.

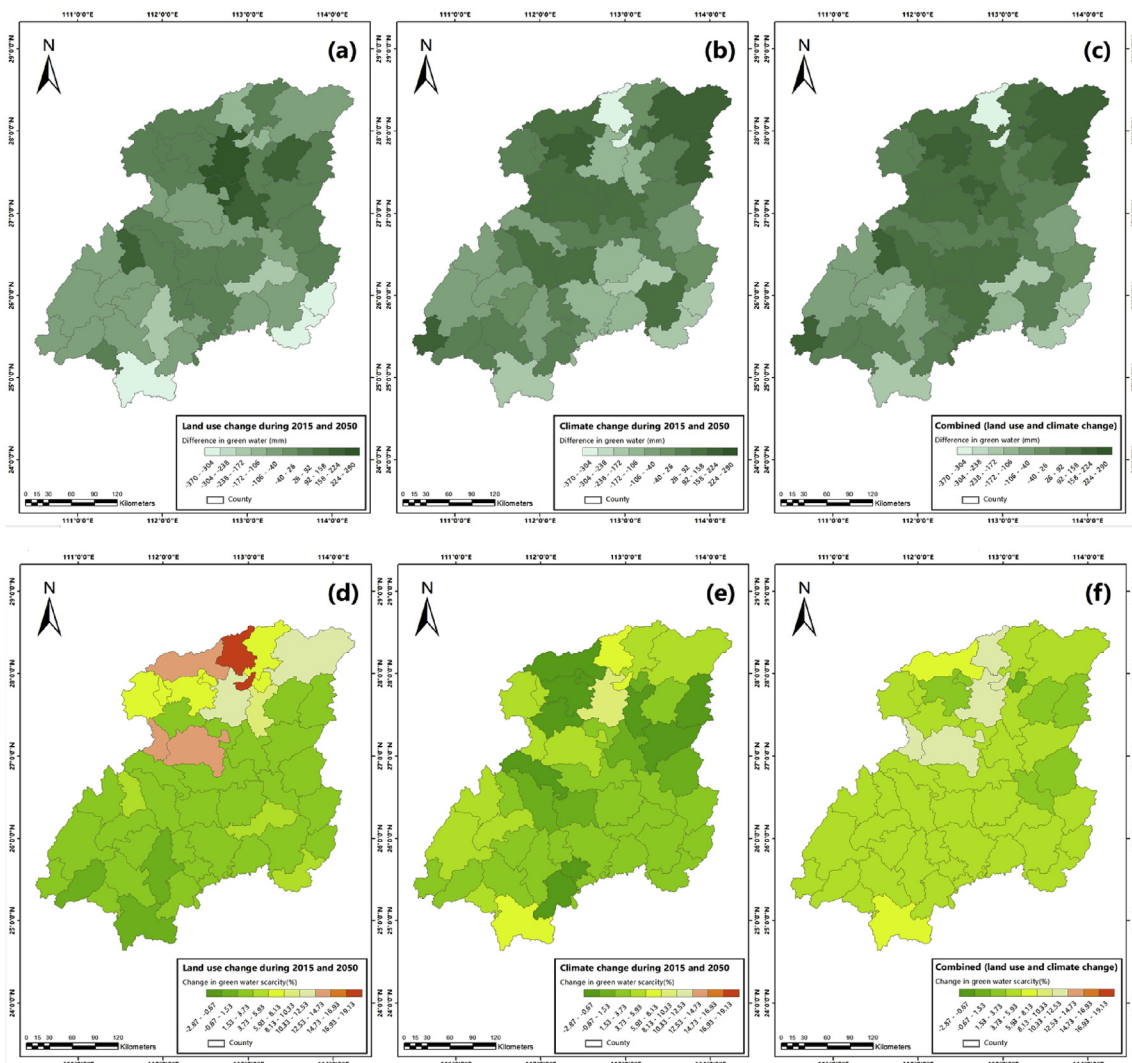


Fig. 4. Changes of the spatial distribution of green water and green water scarcity in Xiangjiang River Basin.

Under future land use and climate scenarios (Fig. 4c), the reduction of GW was mainly distributed in Changsha and Xiangtan in the lower reach. The increase was mainly distributed in Xiangxiang, Liuyang and Pingxiang in the lower reach. For instance, in Xiangxiang, the GW increased 32 mm and 163 mm under land-use change scenario and climate variability scenario, respectively, while the GW increased by 186 mm in the future land use and climate scenario. It might be the comprehensive influence of crop evaporation and precipitation. Land use and climate changes were not a simple synergistic effect on GW changes, which may be the combined effects of urban land, agriculture, precipitation, and temperature (Veetil and Mishra, 2018; Wang et al., 2015).

In this paper, the effects of three scenarios on the spatial distribution of GW-scarcity were analyzed (Fig. 4). The change in GW-scarcity was relatively small, which was lower than the change in BW-scarcity. Under the land-use change scenario (Fig. 4d), the decrease of GW-scarcity was mainly distributed in Guanyang and Jianghua in the upper reach. The increase of GW-scarcity was mainly distributed in Changsha and Xiangtan in the lower reach, and Shaodong, Hengyang in the middle reach. The GW-scarcity of Changsha and Xiangtan increased by 18.38% and 15.36%, respectively. This was due to the increase in urban land and the decrease of agricultural land, resulting in the decrease of the green water availability. Under the climate variability scenario (Fig. 4e), the GW-scarcity change in most of the counties located in the lower and upper reaches was relatively high compared to other areas. For instance, the GW-scarcity in Xiangtan and Jianghua increased by 8.64% and 5.98%, respectively. The main reason may be that the reduction in precipitation decreased the soil water content. Referring to Fig. 4d and e, the spatial variation of GW-scarcity was relatively flat (Fig. 4f). Accordingly, it could be analyzed that urban land, agriculture and precipitation were the three main

environmental factors affecting the GW-scarcity change.

4.4. Factors affecting blue/green water scarcity

The RDA and PCA were used to analyze the correlation between the blue/green water scarcity change and environmental factors (i.e., population, urban land, agriculture, forest, temperature and precipitation) and further determine the main environmental factors affecting the blue/green water scarcity change in each county of XRB. For the RDA method, the characteristic values of axis 1 and axis 2 were 44.2% and 5.83%, respectively (Fig. 5). The explanatory variables of these two axes accounted for 50%, which seven environmental factors could effectively explain the reasons for the blue/green water scarcity change in 49 counties of XRB (Chen et al., 2019). Combined with the PCA, Table 2 listed the correlation coefficients of the above eight indicators. The BW-scarcity was positively correlated with precipitation ($r = 0.425$) and negatively correlated with population ($r = -0.612$). The GW-scarcity was positively correlated with agriculture ($r = 0.429$) and negatively correlated with urban land ($r = -0.593$). It could be seen that precipitation, population, urban land and agriculture had a certain impact on the spatial distribution of BW and GW. These resulted validate sections 4.2 and 4.3.

The results of the CA were shown in the dendrogram (Fig. 7). Five different clusters were obtained at the rescaled distance of 500 on the basis of the standardized values of studied each county in XRB (Tepanosyan et al., 2018). The first and second cluster included Pingxiang, Hengyang and Shaodong in the lower and middle reaches of the XRB (Figs. 1 and 7). The third and fourth cluster included Changsha, Xiangtan, Zhuzhou and other counties in the lower and middle reaches. The fifth cluster included Yongzhou, Chenzhou, Jianghua and other counties in the middle and upper reaches. Thus,

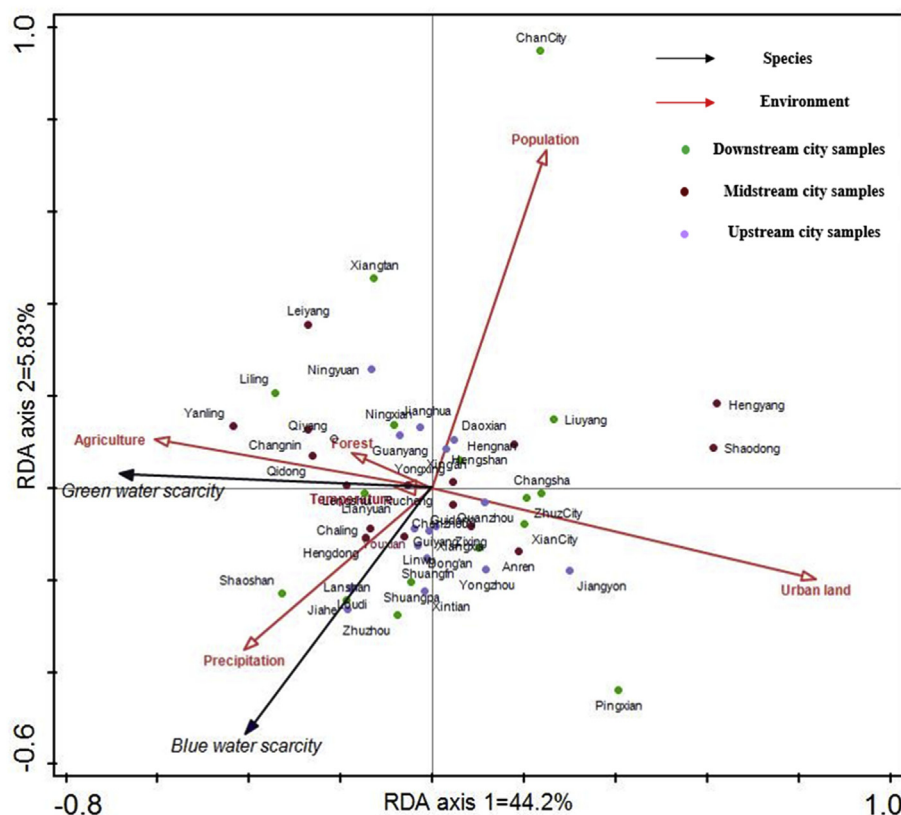


Fig. 5. Results of redundancy analysis describing the relationships between blue/green water scarcity change and the environmental variables.

Table 2

Pearson correlation matrix of blue/green water scarcity, population, urban land, agriculture, forest, precipitation, temperature in Xiangjiang River Basin (n = 49).

	Blue water scarcity	Green water scarcity	Population	urban land	Agriculture	Forest	Precipitation	Temperature
Blue water scarcity	1							
Green water scarcity	0.394	1						
Population	-0.612***	-0.174	1					
urban land	-0.242	-0.593**	0.337	1				
Agriculture	0.202	0.429**	-0.001	-0.292	1			
Forest	0.028	0.124	-0.278	-0.578**	-0.612***	1		
Precipitation	0.425**	0.290	0.165	0.099	0.312	-0.348	1	
Temperature	0.036	0.058	0.252	0.107	0.392	-0.423**	0.285	1

** Correlation is significant at the 0.01 level.
 *** Correlation is significant at the 0.001 level.

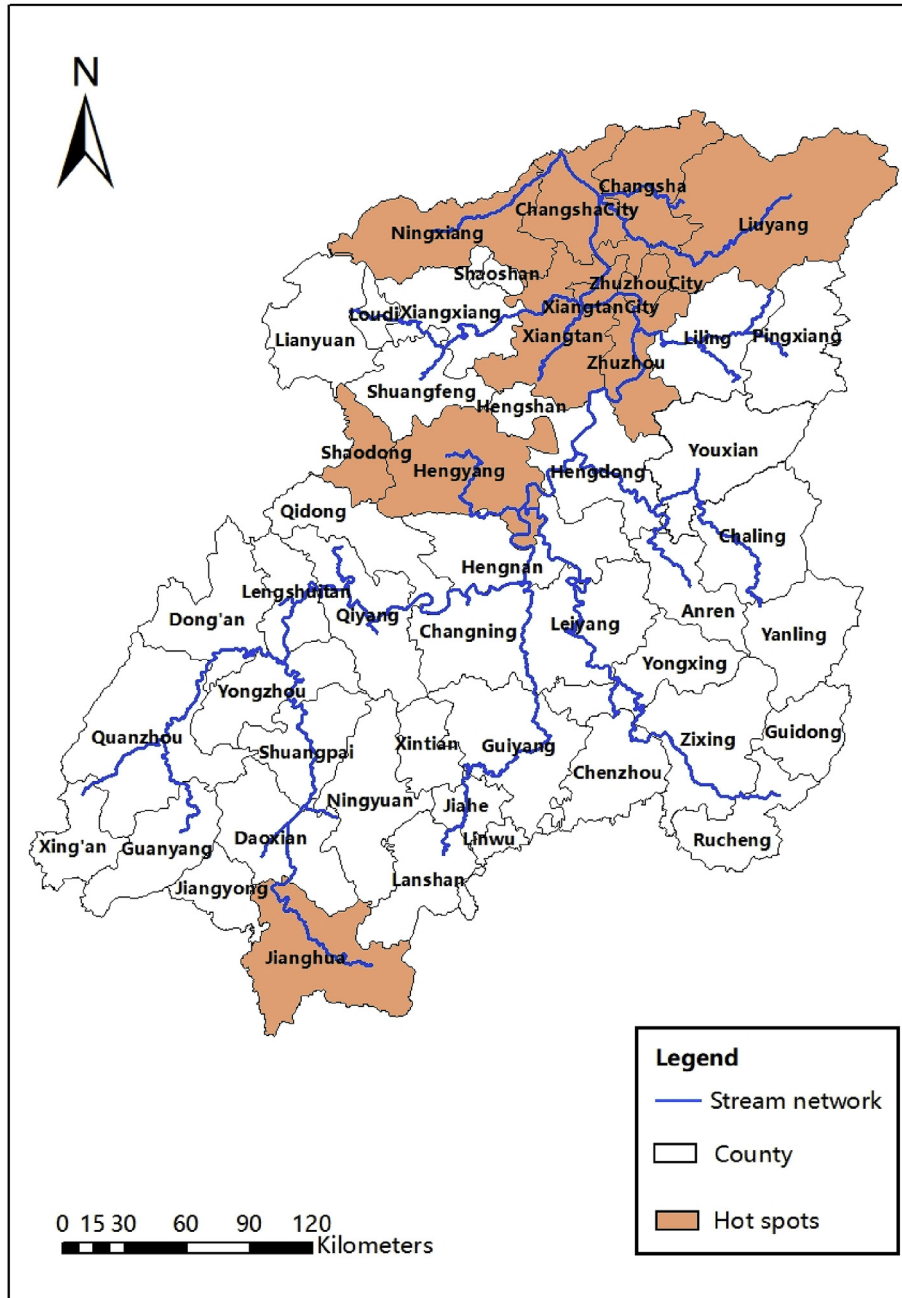


Fig. 6. The hot spots of blue and green water shortage in Xiangjiang River Basin.

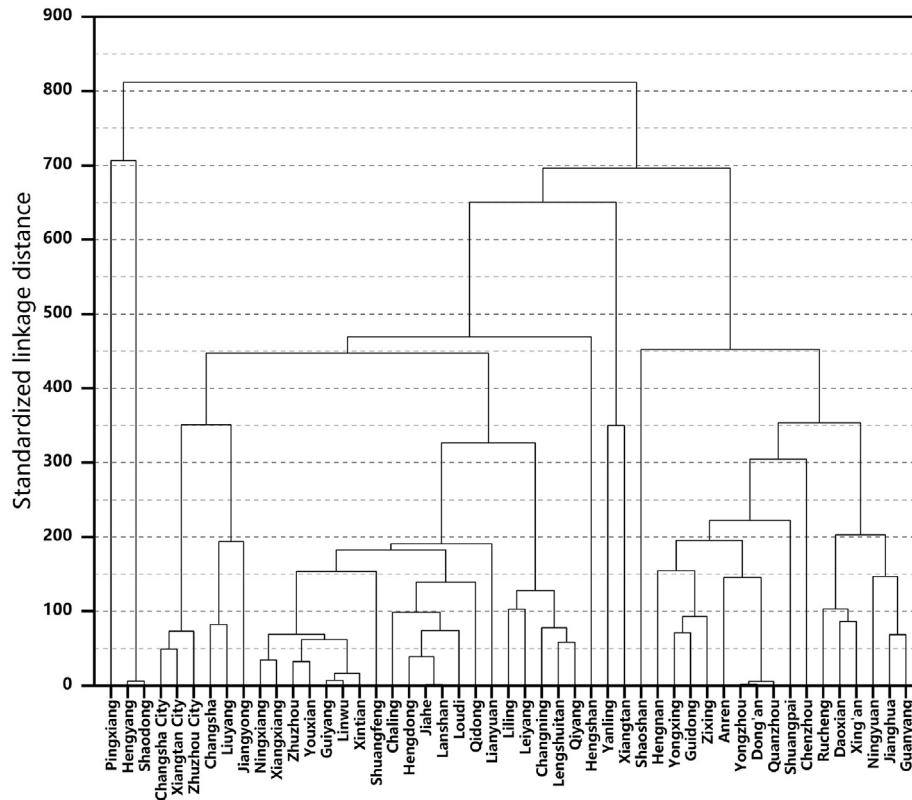


Fig. 7. Dendrogram results from cluster analysis for 49 counties in Xiangjiang River Basin.

it could be seen that the results of CA and RDA were consistent, indicating that the spatial distribution of BW and GW-scarcity change in 49 counties varies with climate and human factors (Tepanosyan et al., 2018). Based on the above analysis, Fig. 6 showed that the hot spot areas of BW and GW shortage accounted for 29.7%, 4.6% and 3.4% of the total area in the lower reach, middle reach and upper reach of XRB, respectively.

4.5. Implications for watershed water resource management

Investigating the influence of climatological and non-climatological drivers simultaneously is essential to understand their complex interactions, and their relative and cumulative impact on BW and GW, which will provide information for water resource management in the future. Shrestha et al. (2017) discovered temperature and precipitation were the two important environmental factors affecting BW and GW in the Athabasca River Basin of Canada. Aparecida et al. (2018) quantified the relative impact of land use change on water resources in two Brazilian basins. In this research, the reserves and utilization of blue/green water resources were inconsistent in each county of the XRB, resulting in different levels of BW and GW-scarcity in each place (Huang et al., 2019). In order to solve this contradiction, it was necessary to discern the key factors affecting BW and GW-scarcity and identify the hotspots of water shortage in the basin. It could help to optimize the allocation of water resources and reduce the risk of water shortages and agricultural drought.

Combined with Figs. 5 and 6, we analyzed the hot spots of BW and GW shortage in Changsha, Xiangtan and Zhuzhou in the lower reach of the XRB; Shaodong and Hengyang in the middle reach; and Jianghua in the upper reach. The critical factors of the spatial distribution of BW and GW were population and urban land in the

lower reach of XRB and the contribution rates were 61.2% and 59.3%, respectively. In the middle reach, the key factor was agriculture land with the contribution rate of 42.9%. In the upper reach, the key factor was precipitation, and the contribution rate was 42.5%. Here were some suggestions for water resources planning in hot spots.

With the growing population in Changsha, Xiangtan and Zhuzhou, the shortage of blue/green water resources was more serious. It needed to properly control the scale of urban expansion and improve the water supply network, so as to alleviate the pressure of water shortage. In Hengyang and Shaodong, the reduction of agriculture and forest aggravated the shortage of GW and government could reasonably planned red lines of ecology and arable land to make the ecosystem sustainable and stable. In Jianghua, due to the influence of reduced precipitation, it was necessary to improve forest coverage and reservoir construction to ensure the safety of local drinking water.

5. Conclusion

For this research, the SWAT model combined with future land use and climate scenarios was successfully applied to quantify the spatiotemporal distribution of blue/green water (scarcity) change for the XRB during 2015 and 2050. It should be noted that most of previous studies on BW and GW were based on scenarios of present land use and climate. There were few studies on future climate and land use changes. Our study is the first attempt to comprehensively evaluate the impacts of future land use and climate changes on the spatiotemporal distribution of blue/green water (scarcity) change using distributed hydrological model and multivariate statistics. The conclusions were as follows:

- (1) As for the results of calibration and validation, the SWAT model performed well at five hydrological stations in the XRB.
- (2) Land use and climate changes were not a simple synergistic effect on blue/green water change. The spatiotemporal changes of BW were principally influenced by the combined effects of urban land, agriculture, forests and precipitation. The spatiotemporal changes of GW were principally influenced by the combined effects of urban land, agriculture, precipitation and temperature.
- (3) The BW-scarcity was mainly affected by precipitation and population, which was positively correlated with precipitation ($r = 0.425$) and negatively correlated with population ($r = -0.612$). The GW-scarcity was mainly affected by agriculture and urban land, which was positively correlated with agriculture ($r = 0.429$) and negatively correlated with urban land ($r = -0.593$).
- (4) We analyzed the hot spots of BW and GW shortage in Changsha, Xiangtan and Zhuzhou in the lower reach of the XRB; Shaodong and Hengyang in the middle reach; and Jianghua in the upper reach. The hot spot areas of BW and GW shortage accounted for 29.7%, 4.6% and 3.4% of the total area in the lower reach, middle reach and upper reach of XRB, respectively.
- (5) In future research work, it is necessary to study the rational allocation of BW and GW resources in the upper and lower reaches of XRB to maximize the use of the resources.

This study would help regional watershed managers to make reasonable decisions on water resources management and protection in the XRB. It could also provide reference for the study of water resources in other basins.

Declaration of competing interest

The authors declare that they have no known competing financial interests or personal relationships that could have appeared to influence the work reported in this paper.

CRediT authorship contribution statement

Jie Liang: Writing - review & editing, Conceptualization, Methodology. **Qiang Liu:** Writing - original draft, Software, Data curation. **Hua Zhang:** Writing - review & editing, Software. **Xiaodong Li:** Writing - review & editing. **Zhan Qian:** Data curation. **Manqin Lei:** Data curation. **Xin Li:** Data curation. **Yuhui Peng:** Data curation. **Shuai Li:** Data curation. **Guangming Zeng:** Data curation.

Acknowledgments

This work was supported by the Natural Science Foundation of Hunan Province (2019JJ20002), the National Natural Science Foundation of China (51679082, 51479072, 51979101, 51521006), the Hunan Science & Technology Innovation Program (2018RS3037), the Three Gorges Follow-up Research Project (2017HXXY-05), and China Scholarship Council (201806135015).

Appendix A. Supplementary data

Supplementary data to this article can be found online at <https://doi.org/10.1016/j.jclepro.2020.121834>.

References

An, Q., Wu, Q., Li, J., Xiong, B., Chen, X., 2019. Environmental efficiency evaluation

- for Xiangjiang River basin cities based on an improved SBM model and Global Malmquist index. *Energy Econ.* 81, 95–103.
- Aparecida, D.H.T., Vale, S.F., Eugênio, A.S.J., 2018. Assessment of the recent land use change dynamics related to sugarcane expansion and the associated effects on water resources availability. *J. Clean. Prod.* 197, 1328–1341.
- Awan, U.K., Ismaeel, A., 2014. A new technique to map groundwater recharge in irrigated areas using a SWAT model under changing climate. *J. Hydrol.* 519, 1368–1382.
- Charles, A.L., Alamsjah, M.A., 2019. Application of chemometric techniques: an innovative approach to discriminate two seaweed cultivars by physico-functional properties. *Food Chem.* 289, 269–277.
- Chen, B., Tan, S., Zeng, Q., Wang, A., Zheng, H., 2019. Soil nutrient heterogeneity affects the accumulation and transfer of cadmium in Bermuda grass (*Cynodon dactylon* (L.) pers.). *Chemosphere* 221, 342–348.
- Chen, H., Luo, Y., Potter, C., Moran, P.J., Grieneisen, M.L., Zhang, M., 2017. Modeling pesticide diuron loading from the san joaquin watershed into the sacramento-san joaquin delta using SWAT. *Water Res.* 121, 374–385.
- Chen, X., Yi, G., Liu, J., Liu, X., Chen, Y., 2018. Evaluating economic growth, industrial structure, and water quality of the Xiangjiang River Basin in China based on a spatial econometric approach. *Int. J. Environ. Res. Publ. Health* 15 (10), 2095.
- Cheng, Z., Chen, L., Li, H., Lin, J., Yang, Z., Yang, Y., Xu, X., Xian, J., Shao, J., Zhu, X., 2018. Characteristics and health risk assessment of heavy metals exposure via household dust from urban area in Chengdu, China. *Sci. Total Environ.* 619, 621–629.
- Du, L., Rajib, A., Merwade, V., 2018. Large scale spatially explicit modeling of blue and green water dynamics in a temperate mid-latitude basin. *J. Hydrol.* 562, 84–102.
- Faramarzi, M., Abbaspour, K.C., Ashraf Vaghefi, S., Farzaneh, M.R., Zehnder, A.J.B., Srinivasan, R., Yang, H., 2013. Modeling impacts of climate change on freshwater availability in Africa. *J. Hydrol.* 480, 85–101.
- Faramarzi, M., Abbaspour, K.C., Schulin, R., Yang, H., 2009. Modelling blue and green water resources availability in Iran. *Hydrol. Processes* 23 (3), 486–501.
- Giri, S., Arbab, N.N., Lathrop, R.G., 2018. Water security assessment of current and future scenarios through an integrated modeling framework in the Neshanic River Watershed. *J. Hydrol.* 563, 1025–1041.
- Geospatial data Cloud. <http://www.gscloud.cn/>, 2018.
- Hoekstra, A.Y., Mekonnen, M.M., 2012. The water footprint of humanity. *Proc. Natl. Acad. Sci. U. S. A.* 109 (9), 3232–3237.
- Hou, H., Wang, R., Murayama, Y., 2019. Scenario-based modelling for urban sustainability focusing on changes in cropland under rapid urbanization: a case study of Hangzhou from 1990 to 2035. *Sci. Total Environ.* 661, 422–431.
- Hua, S., Liang, J., Zeng, G., Xu, M., Zhang, C., Yuan, Y., Li, X., Li, P., Liu, J., Huang, L., 2015. How to manage future groundwater resource of China under climate change and urbanization: an optimal stage investment design from modern portfolio theory. *Water Res.* 85, 31–37.
- Huang, Z., Hejazi, M., Tang, Q., Vernon, C.R., Liu, Y., Chen, M., Calvin, K., 2019. Global agricultural green and blue water consumption under future climate and land use changes. *J. Hydrol.* 574, 242–256.
- Johansson, E.L., Fader, M., Seaquist, J.W., Nicholas, K.A., 2016. Green and blue water demand from large-scale land acquisitions in Africa. *Proc. Natl. Acad. Sci. U. S. A.* 113 (41), 11471–11476.
- Liang, J., He, X., Zeng, G., Zhong, M., Gao, X., Li, X., Li, X., Wu, H., Feng, C., Xing, W., 2018. Integrating priority areas and ecological corridors into national network for conservation planning in China. *Sci. Total Environ.* 626, 22–29.
- Liang, J., Zeng, G., Guo, S., Li, J., Wei, A., Shi, L., Li, X., 2009. Uncertainty analysis of stochastic solute transport in a heterogeneous aquifer. *Environ. Eng. Sci.* 26 (2), 359–368.
- Liang, J., Zhong, M., Zeng, G., Chen, G., Hua, S., Li, X., Yuan, Y., Wu, H., Gao, X., 2016. Risk management for optimal land use planning integrating ecosystem services values: a case study in Changsha, Middle China. *Sci. Total Environ.* 579, 1675–1682.
- Liu, Y., Lu, Y., Fu, B., Harris, P., Wu, L., 2019. Quantifying the spatio-temporal drivers of planned vegetation restoration on ecosystem services at a regional scale. *Sci. Total Environ.* 650, 1029–1040.
- Masud, M.B., Wada, Y., Goss, G.G., Faramarzi, M., 2019. Global implications of regional grain production through virtual water trade. *Sci. Total Environ.* 659, 807–820.
- Mou, L.T., Ibrahim, A.L., Yusop, Z., Chua, V.P., Chan, N.W., 2017. Climate change impacts under CMIP5 RCP scenarios on water resources of the Kelantan River Basin, Malaysia. *Atmos. Res.* 189, 1–10.
- Nilawar, A.P., Waikar, M.L., 2019. Impacts of climate change on streamflow and sediment concentration under RCP 4.5 and 8.5: a case study in Purna river basin, India. *Sci. Total Environ.* 650, 2685–2696.
- Niraula, R., Meixner, T., Norman, L.M., 2015. Determining the importance of model calibration for forecasting absolute/relative changes in streamflow from LULC and climate changes. *J. Hydrol.* 522, 439–451.
- Noori, N., Kalin, L., 2015. Coupling SWAT and ANN models for enhanced daily streamflow prediction. *J. Hydrol.* 533, 141–151.
- Rodrigues, D.B.B., Gupta, H.V., Mendiando, E.M., 2015. A blue/green water-based accounting framework for assessment of water security. *Water Resour. Res.* 50 (9), 7187–7205.
- Rost, S., Gerten, D., Bondeau, A., Lucht, W., Rohwer, J., Schaphoff, S., 2008. Agricultural green and blue water consumption and its influence on the global water system. *Water Resour. Res.* 44 (9).
- Schulz, J., Abbaspour, K.C., Srinivasan, R., Yang, H., 2008. Estimation of freshwater

- availability in the West African sub-continent using the SWAT hydrologic model. *J. Hydrol* 352 (1), 30–49.
- Schyns, J.F., Hoekstra, A.Y., Booij, M.J., 2015. Review and classification of indicators of green water availability and scarcity. *Hydrol. Earth Syst. Sci.* 12 (4), 5519–5564.
- Shrestha, N.K., Du, X., Wang, J., 2017. Assessing climate change impacts on fresh water resources of the Athabasca River Basin, Canada. *Sci. Total Environ.* 601, 425–440.
- Tepanosyan, G., Sahakyan, L., Belyaeva, O., Asmaryan, S., Saghatelian, A., 2018. Continuous impact of mining activities on soil heavy metals levels and human health. *Sci. Total Environ.* 639, 900–909.
- Tuo, Y., Marcolini, G., Disse, M., Chiogna, G., 2018. A multi-objective approach to improve SWAT model calibration in alpine catchments. *J. Hydrol* 559, 347–360.
- Veettil, A.V., Mishra, A.K., 2016. Water security assessment using blue and green water footprint concepts. *J. Hydrol* 542, 589–602.
- Veettil, A.V., Mishra, A.K., 2018. Potential influence of climate and anthropogenic variables on water security using blue and green water scarcity, Falkenmark index, and freshwater provision indicator. *J. Environ. Manag.* 228, 346–362.
- Veldkamp, T.I.E., Wada, Y., Aerts, J.C.J.H., Döll, P., Gosling, S.N., Liu, J., Masaki, Y., Oki, T., Ostberg, S., Pokhrel, Y., 2017. Water scarcity hotspots travel downstream due to human interventions in the 20th and 21st century. *Nat. Commun.* 8, 15697.
- Wang, Q., Liu, R., Men, C., Guo, L., Miao, Y., 2019. Temporal-spatial analysis of water environmental capacity based on the couple of SWAT model and differential evolution algorithm. *J. Hydrol* 569, 155–166.
- Wang, R., Kalin, L., Kuang, W., Tian, H., 2015. Individual and combined effects of land use/cover and climate change on wolf bay watershed streamflow in southern Alabama. *Hydrol. Process.* 28 (22), 5530–5546.
- Xu, Y., Zhang, X., Ran, Q., Tian, Y., 2013. Impact of climate change on hydrology of upper reaches of Qiantang River Basin, East China. *J. Hydrol* 483, 51–60.
- Xue, L., Zhu, B., Wu, Y., Wei, G., Liao, S., Yang, C., Wang, J., Zhang, H., Ren, L., Han, Q., 2019. Dynamic projection of ecological risk in the Manas River basin based on terrain gradients. *Sci. Total Environ.* 653, 283–293.
- Yuan, Z., Xu, J., Meng, X., Wang, Y., Yan, B., Hong, X., 2019. Impact of climate variability on blue and green water flows in the erhai lake Basin of southwest China. *Water* 11 (3), 424.
- Zang, C.F., Liu, J., Der Velde, M.V., Kraxner, F., 2012. Assessment of spatial and temporal patterns of green and blue water flows under natural conditions in inland river basins in Northwest China. *Hydrol. Earth Syst. Sci.* 16 (8), 2859–2870.
- Zhao, A., Zhu, X., Liu, X., Pan, Y., Zuo, D., 2016. Impacts of land use change and climate variability on green and blue water resources in the Weihe River Basin of northwest China. *Catena* 137, 318–327.
- Zhou, F., Xu, Y., Chen, Y., Xu, C.-Y., Gao, Y., Du, J., 2013. Hydrological response to urbanization at different spatio-temporal scales simulated by coupling of CLUE-S and the SWAT model in the Yangtze River Delta region. *J. Hydrol* 485, 113–125.
- Zuo, D., Xu, Z., Peng, D., Song, J., Lei, C., Wei, S., Abbaspour, K.C., Hong, Y., 2015. Simulating spatiotemporal variability of blue and green water resources availability with uncertainty analysis. *Hydrol. Process.* 29 (8), 1942–1955.
- Zuo, D., Xu, Z., Yao, W., Jin, S., Xiao, P., Ran, D., 2016. Assessing the effects of changes in land use and climate on runoff and sediment yields from a watershed in the Loess Plateau of China. *Sci. Total Environ.* 544, 238–250.